AIMS Materials Science, 3(2): 448-459.
DOI: 10.3934/matersci.2016.2.448
Received: 18 January 2016
Accepted: 28 March 2016
Published: 05 April 2016

http://www.aimspress.com/journal/Materials

Research article

Electrochemical impedance spectroscopy analysis with a symmetric cell for $LiCoO_2$ cathode degradation correlated with Co dissolution

Hiroki Nara [1], Keisuke Morita [2], Tokihiko Yokoshima [1], Daikichi Mukoyama [1], Toshiyuki Momma [1,2], and Tetsuya Osaka [1,2,*]

[1] Research Institute for Science and Engineering, Waseda University, 3-4-1, Okubo, Shinjuku-ku, Tokyo 169-8555, Japan
[2] Graduate School of Science and Engineering, Waseda University, 3-4-1, Okubo, Shinjuku-ku, Tokyo 169-8555, Japan

* **Correspondence:** Email: osakatets@waseda.jp; Tel: +81-3-5286-3202; Fax: +81-3-3205-2074.

Abstract: Static degradation of $LiCoO_2$ cathodes is a problem that hinders accurate analysis using our developed separable symmetric cell. Therefore, in this study we investigate the static degradation of $LiCoO_2$ cathodes in separable symmetric cells by electrochemical impedance spectroscopy (EIS) and inductively coupled plasma analyses. EIS measurements of $LiCoO_2$ cathodes are conducted in various electrolytes, with different anions and with or without HF and/or H_2O. This allows us to determine the static degradation of $LiCoO_2$ cathodes relative to their increase of charge transfer resistance. The increase of the charge transfer resistance of the $LiCoO_2$ cathodes is attributed to cobalt dissolution from the active material of $LiCoO_2$. Cobalt dissolution from $LiCoO_2$ is revealed to occur even at low potential in the presence of HF, which is generated from $LiPF_6$ and H_2O. The results indicate that avoidance of HF generation is important for the analysis of lithium-ion battery electrodes by using the separable cell. These findings reveal the condition to achieve accurate analysis by EIS using the separable cell.

Keywords: electrochemical impedance spectroscopy (EIS); Lithium-ion Battery (LIB); $LiCoO_2$ cathode; degradation; Co dissolution; $LiPF_6$; $LiClO_4$; HF

1. Introduction

Since the launch of lithium-ion batteries (LIBs) into the market in 1991 [1], LIBs have been

widely used in portable electric devices owing to their higher power and energy density compared with other batteries. Recently, the application of LIBs has been expanded to hybrid electric vehicles (HEVs) and battery electric vehicles (BEVs), to exploit their high efficiency energy usage [2]. LIBs have been further proven to be useful in innovative technology, such as smart grids [3,4]. Thus, LIBs are one of the most important devices for a sustainable society. Given that rechargeable batteries, including LIBs, store and deliver electricity through chemical reactions, the batteries degrade with charge–discharge cycles and storage time [5]. The degradation of LIBs has been widely investigated; for anodes, formation of a solid electrolyte interphase (SEI) increases the internal resistance of LIBs [5,6] and metallic lithium deposition on the anode lowers their safety of LIBs [7]. For cathodes, surface film formation increases internal resistance [8,9] and dissolution of transition metal dissolution degrade their capacity [6]. Therefore, the diagnostic technology of LIBs is important, not only for research and development, but also for application in HEVs, BEVs, and smart grids.

Electrochemical impedance spectroscopy (EIS) is a powerful tool for in-situ measurement without having to disassemble the battery. It is also beneficial in that it can separate a complicated reaction process into elementary processes on the basis of the difference in time constants. Hence, the degraded part and degree in a LIB can be interpreted on the basis of the elementary processes by means of EIS. Therefore, EIS has been extensively applied in this field [6,10–23]. However, because information acquired from both the cathode and anode is complex, it is still difficult for impedance analysis to evaluate LIBs accurately. In addition, the recent development of LIBs has made the impedance values smaller and the time constants for the processes closer, which have resulted in the overlapping of the impedance responses [23,24]. Therefore, the cathode and anode should be analyzed separately, before the impedance response of the whole LIB can be assessed. To separate the impedance response of LIBs, many researchers have adopted the approach to use a reference electrode such as lithium foil [25,26], Li_xAl micro wire [27], Li_ySn micro wire [28], $Li_4Ti_5O_{12}$ or $LiFePO_4$ [29] and lithiated bismuth [30]. However, although a reference electrode should be theoretically inserted between the cathode and anode [22], the insertion of a reference electrode between the cathode and anode may cause difficulties by disturbing the uniform current distribution between the electrodes. However, the impedance response, which is obtained by a reference electrode placed away from the middle of the electrodes, is strongly influenced by the potential gradient [31,32]. Therefore, the edges of cathode and anode must align completely, otherwise the potential gradient away from the opposing electrodes will vary during frequency sweep of input amplitude in impedance measurement.

To accurately determine the impedance of the cathode and anode, we developed a separable cell, which consisted of two electrode sheets that were 70 mm × 70 mm in size, which were compatible to configure a 5 Ah class pouch type LIB cell. The separable cell was mounted in electrode holders with an optional separation gap of electrodes, which enabled a change of electrodes between electrochemical measurements [33]. The possibility to measure an impedance accurately by using a symmetric cell has been explained by Chen et al. [34] and Aurbach et al. [35]. In our previous study [33], the impedance, which was obtained from the symmetric cell of $LiCoO_2$ cathodes with an electrolyte composed of 1.0 mol/dm^3 $LiPF_6$ in a 1:1 mixture of ethylene carbonate (EC) and diethyl carbonate (DEC) (1 M $LiPF_6$/EC-DEC) containing less than 20 ppm of H_2O without any additives, obviously increased with storage time after the symmetric cell assembly from full cells, while that of graphite anodes did not change, as shown in Fig. 2. The degradation of the $LiCoO_2$ cathode was well-investigated by Aurbach et al. [9] by means of inductively coupled plasma mass spectrometry

(ICP-MS), X-ray photoelectron spectroscopy, and EIS. According to the literature, the $LiCoO_2$ cathode degrades on its surface rather than its bulk: on the surface, LiF, which is a product of the reaction between $LiCoO_2$ and HF, was detected. However, the conclusion remained that "the presence of HF in solutions may play a major negative role" [9], while cobalt dissolution from $LiCoO_2$ at high voltage was reported by Amatucci et al. [36].

Herein, we investigate the $LiCoO_2$ cathode degradation at the relatively low potential of 3.7 V, which was detected by EIS using the separable cell, and correlated that with Co dissolution by changing the electrolyte conditions which relates to HF generation.

2. Materials and Method

A full pouch-type LIB cell fabricated in a dry room maintained a dew point below −50 °C in the laboratory used in this work. The full LIB cell was composed of a $LiCoO_2$ cathode with a capacity of 1.5 mA cm^{-2}, and a carbon anode with a capacity of 1.6 mAh cm^{-2} with the electrode areas of 46.24 cm^2 and 49.00 cm^2 for cathode and anode, respectively, after being dried in a vacuum at 120 °C for 2 hours. The electrolyte used was 1 M $LiPF_6$/EC-DEC containing less than 20 ppm of H_2O in a polyolefin separator without any additives.

The pouch-type cells were charged and discharged in two initial cycles between 3.0 and 4.2 V at a rate of 0.1 C (7.0 mA) as the aging process to stabilize the cell performance, and were maintained at 4.2 V for 1 h at the end of each charge process before starting the electrochemical investigation or charge/discharge cycling test. All the pouch type cells exhibited an initial discharge capacity of 42 ± 1 mAh at the second cycle during the aging process as shown in Fig. 1.

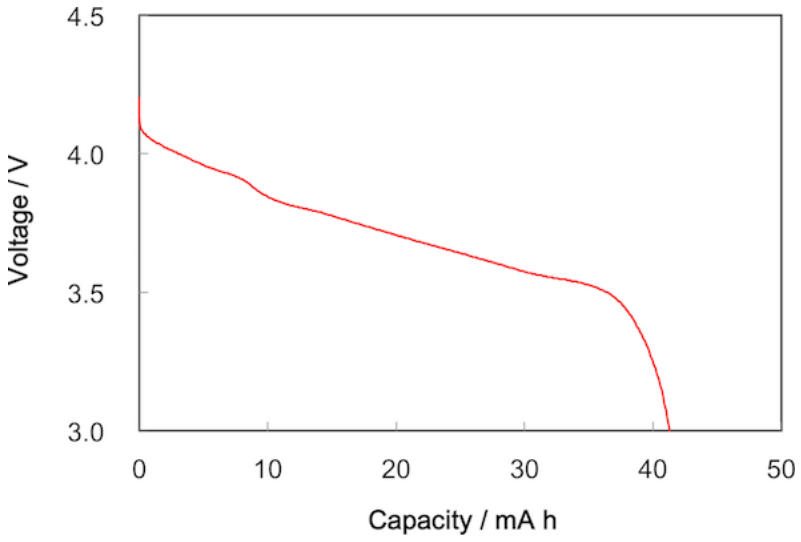

Figure 1. Discharge curve of a pouch-type cell just before disassembly to form a symmetric cell.

Symmetric cells, which contained two identical electrodes, were configured using two cathode sheets or two anode sheets for the investigation. The two sets of identical cathodes and identical anodes were prepared from two pouch-type cells, which were charged and discharged in pairs. For the EIS analysis of the symmetric cells, the cells were charged up to 3.7 V after the aging process and then EIS was performed.

When opening these two pouch-type cells, which were operated under the same conditions, the cathodes and anodes were taken out from the cell, and were removed from the separators used in the pouch-type cells. To configure the symmetric cells, a separable cell module [33] was used. This module enabled the handling of large electrode sheets, 68 mm × 68 mm for cathodes and 70 mm × 70 mm for anodes. Two sheets of cathodes were mounted to electrode holders that were designed to maintain the shape of the sheets with an electric conducting path from the current collector sheet to the outer lead. The electrode holders mounted with cathodes were faced towards each other with a spacer frame to maintain a 10 mm gap with sealing, and then fresh electrolyte solutions were poured to fill the space between the electrodes to complete the cathode symmetric cell. An anode symmetric cell was also formed in the same manner with two anode sheets obtained from the two whole LIB cells. The reassembling of the cells was performed in a dry Ar-filled glove box. In the present study, four electrolytes were used as the fresh electrolyte solutions, 1 M $LiPF_6$/EC-DEC, 1 M $LiClO_4$/EC-DEC, 1 M $LiClO_4$/EC-DEC with 100 ppm of aqueous HF, and 1 M $LiClO_4$/EC-DEC with 50 ppm of H_2O.

The AC impedance spectra were obtained at the open circuit voltage with 20 mV (peak to peak) of an AC signal in the frequency range of 100 kHz to 10 mHz using a potentiostat system (VSP, Bio Logic, Claix, France) with elapsed time from assembly of the symmetric cells. All measurements were performed at room temperature. The impedance spectra are shown as a sum of two identical cathodes and two identical anodes, and all Nyquist plots are aligned with the intersections of the plots and x-axis by subtracting the resistances, which are generally related to the electrolyte solution, electric contacts, and wiring.

The Co concentration in the electrolyte solutions was analyzed by the ICP technique (ICP-MS, Agilent 7700, Agilent Technologies, Santa Clara, CA, United States). A small amount of the electrolyte solutions was extracted from the symmetric cells at each elapsed time from the assembly of the symmetric cells.

3. Results and Discussion

Figure 2 shows the Nyquist and Bode plots of the impedances obtained in 1 M $LiPF_6$/EC-DEC with the elapsed time from assembly of the cathode and anode symmetric cells. The impedance response of the $LiCoO_2$ cathode in the Nyquist plots has two semi-circles with characteristic frequencies observed at approximately 1 kHz and 1 Hz: the former semi-circle is difficult to be determined because of the very small impedance compared with the latter semi-circle and an inductive response at the high frequency region. In the literature, the two semicircles in the cathode were confirmed at a several kHz and a several Hz, which were attributed to lithium migration in the surface film and charge transfer, respectively [37]. As for the impedance of the $LiCoO_2$ cathode, it is revealed that the charge transfer resistance obviously increased with the elapsed time. The increase rate of the charge transfer resistance after 3, 6, and 24 hours are roughly calculated to be 2.4, 3.4, and 7.0, respectively. However, the impedance response of the graphite anode in the Nyquist plots has two semi-circles overlapping whose characteristic frequency was observed at approximately 1 kHz. In our previous work, the overlapping semicircles in the anode contains at least two elemental processes, which are lithium migration in a solid electrolyte interphase (SEI) and charge transfer [38,39]. In contrast to the impedance of the $LiCoO_2$ cathode, the graphite anode impedance with elapsed time was hardly observed at the frequency regions in which the lithium migration in a

SEI and charge transfer occur. The increase of the $LiCoO_2$ cathode impedance is in accordance with the previous study [9]. The previous study explained that the degradation of the $LiCoO_2$ cathode may be the effect of HF that is generated from the reaction of $LiPF_6$ and H_2O as indicated in Eq. (1). Therefore, we selected $LiClO_4$ as a lithium salt instead of $LiPF_6$ to exclude the HF source.

$$PF_6^- + H_2O \rightarrow HF + PF_5 + OH^- \quad (1)$$

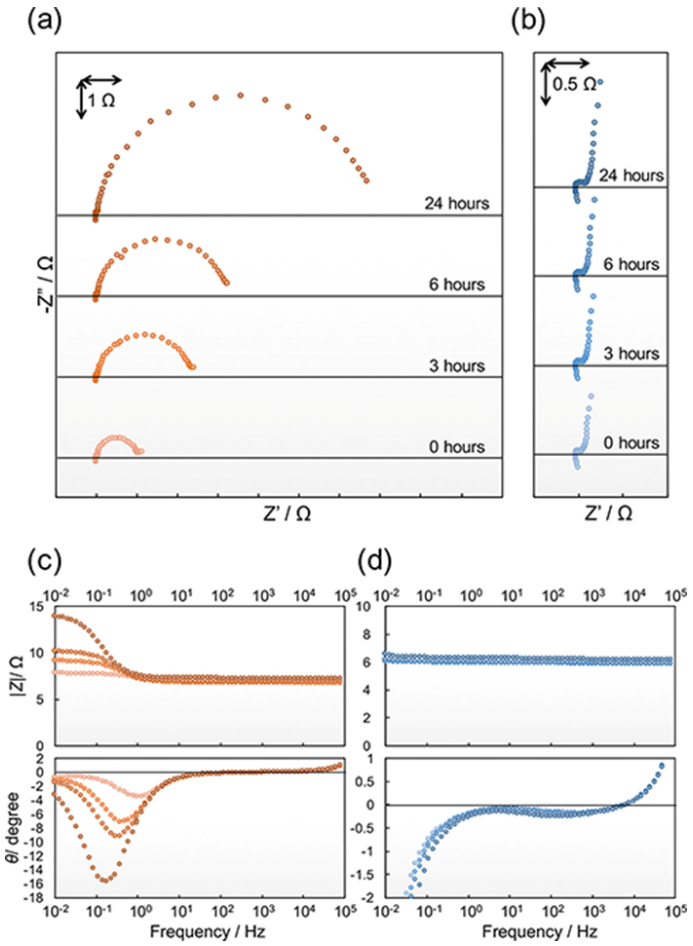

Figure 2. Nyquist and Bode plots of the impedances obtained in 1 M $LiPF_6$/EC-DEC with elapsed time from the assembly of the (a) and (c) cathode symmetric cell, and (b) and (d) anode symmetric cell.

Figure 3 shows the Nyquist and Bode plots of the impedances obtained in 1 M $LiClO_4$/EC-DEC with elapsed time from the assembly of cathode and anode symmetric cells. As was the case with 1 M $LiPF_6$/EC-DEC, the impedance response of the $LiCoO_2$ cathode in the Nyquist plots have two semi-circles whose maxima were observed at approximately 1 kHz and 1 Hz, and the impedance response of the graphite anode in the Nyquist plots have two semicircles overlapping whose maximum was observed at approximately 1 kHz. However, as for the impedance of the $LiCoO_2$ cathode, an increase of the charge transfer resistance with the elapsed time was not confirmed, compared with the case of 1 M $LiPF_6$/EC-DEC. The increase rate of the charge transfer resistance after 3, 6, and 24 hours were roughly calculated to be 1.1, 1.2, and 1.4, respectively. However, the

impedance of the graphite anode was not changed at the frequency region in which the lithium migration in a SEI and the charge transfer occur, as was observed in the case of 1 M $LiPF_6$/EC-DEC. Therefore, the difference between 1 M $LiPF_6$/EC-DEC and 1 M $LiClO_4$/EC-DEC for the charge transfer resistance of $LiCoO_2$ is considered to be derived from the effect of HF, as was discussed by Aurbach et al. [9].

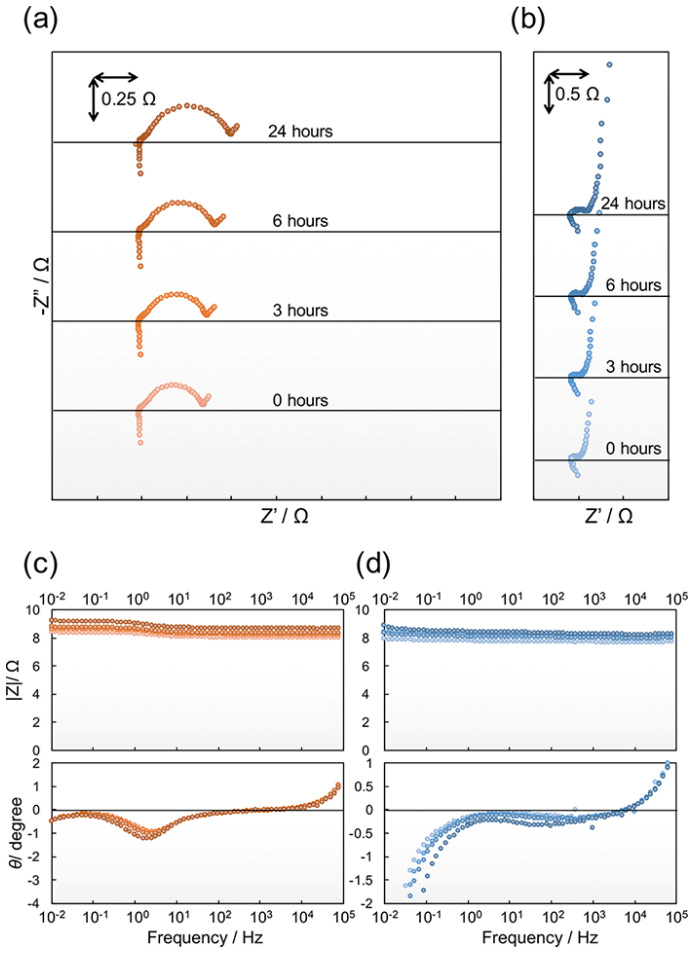

Figure 3. Nyquist and Bode plots of the impedances obtained in 1 M $LiClO_4$/EC-DEC with elapsed time from the assembly of the (a) and (c) cathode symmetric cell, and (b) and (d) the anode symmetric cell.

To confirm the effect of HF, we investigated the Co concentration in the electrolyte of the cathode symmetric cells by ICP-MS with the elapsed time. The cobalt concentration variation in the electrolyte of 1 M $LiPF_6$/EC-DEC and 1 M $LiClO_4$/EC-DEC with elapsed time is shown in Figure 4. The effect of HF is clearly confirmed to be responsible for the cobalt dissolution. The cobalt concentration in the electrolyte of 1 M $LiPF_6$/EC-DEC increased with the elapsed time, whereas that of 1 M $LiClO_4$/EC-DEC was approximately constant. The results suggest that the increase of the charge transfer resistance of $LiCoO_2$ strongly relates to the cobalt dissolution by HF. In contrast, X-ray photon spectroscopy of the $LiCoO_2$ cathode surfaces in 1 M $LiPF_6$/EC-DEC and 1 M $LiClO_4$/EC-DEC did not reveal any obvious difference (data not shown). Additionally, according to a paper by D. Aurbach et al. [9], the XRD patterns of $LiCoO_2$ samples cycled or stored at 25 ºC were

identical even though the samples possessed different impedances.

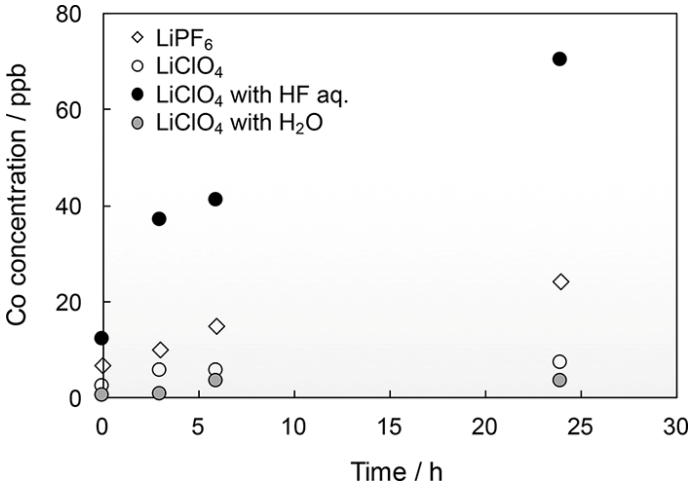

Figure 4. Cobalt concentration variation in the electrolytes of 1 M $LiPF_6$/EC-DEC, 1 M $LiClO_4$/EC-DEC, 1 M $LiClO_4$/EC-DEC with 100 ppm aqueous HF, and 1 M $LiClO_4$/EC-DEC with 100 ppm H_2O with elapsed time from the assembly of the symmetric cells.

To establish the effect of HF, HF solution was added to the electrolyte of 1 M $LiClO_4$/EC-DEC, in which there are no HF sources. Figure 5 shows the Nyquist and Bode plots of the impedances obtained in 1 M $LiClO_4$/EC-DEC with 100 ppm of aqueous HF with elapsed time from the assembly of the cathode and anode symmetric cells. As was the case with 1 M $LiPF_6$/EC-DEC, the impedance response of the $LiCoO_2$ cathode in Nyquist plots has two semi-circles whose characteristic frequencies were observed at approximately 1 kHz and 1 Hz, and the impedance response of the graphite anode in Nyquist plots have two semi-circles overlapping whose characteristic frequency was observed at approximately 1 kHz. Additionally, as was observed for the impedance of the $LiCoO_2$ cathode, the increase of the charge transfer resistance with the elapsed time was confirmed. The increase rate of the charge transfer resistance after 3, 6, and 24 hours are roughly calculated to be 2.0, 2.4, and 3.6, respectively. Additionally, the cobalt concentration variation in the electrolyte of 1 M $LiClO_4$/EC-DEC with 100 ppm aqueous HF clearly shows the relationship with HF, as shown in Fig. 4. The cobalt concentration in the 1 M $LiClO_4$/EC-DEC electrolyte with 100 ppm aqueous HF increased with elapsed time. However, the impedance of the graphite anode was unchanged at the frequency region in which the lithium migration in a SEI and the charge transfer occur. The result confirms the effect of HF to increase the charge transfer resistance of $LiCoO_2$. Here, one should consider the role of the water in the HF solution.

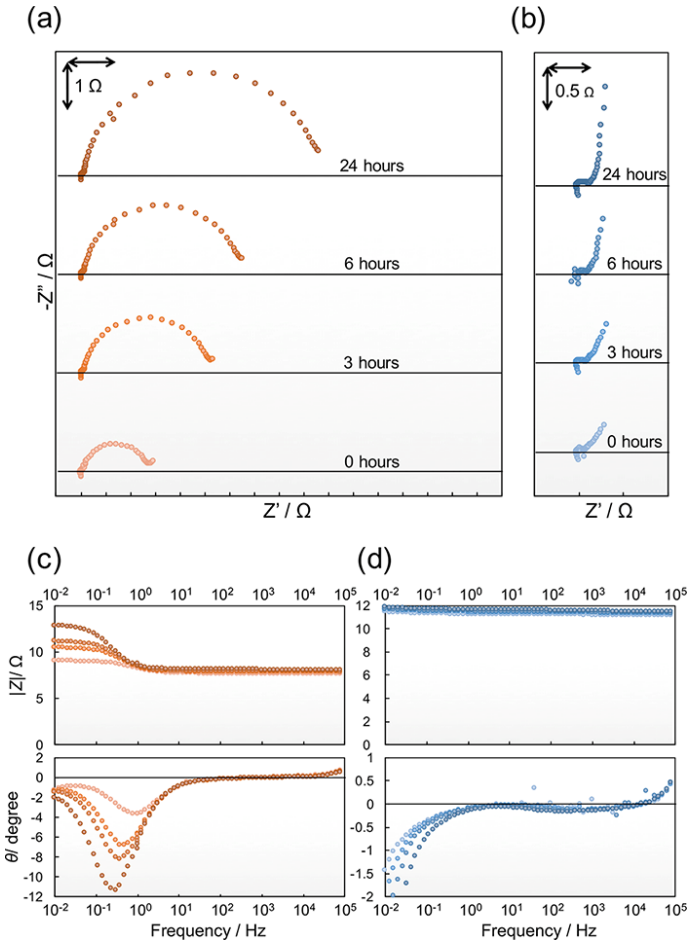

Figure 5. Nyquist and Bode plots of the impedances obtained in 1 M $LiClO_4$/EC-DEC with 100 ppm aqueous HF with elapsed time from the assembly of the (a) and (c) cathode symmetric cell, and (b) and (d) anode symmetric cell.

To eliminate a role of the water in the HF solution, distilled water was added to the 1 M $LiClO_4$/EC-DEC electrolyte. Figure 6 shows the Nyquist and Bode plots of the impedances obtained in 1 M $LiClO_4$/EC-DEC with 50 ppm H_2O with elapsed time from the assembly of the cathode and anode symmetric cells. As was the case with 1 M $LiPF_6$/EC-DEC and 1 M $LiClO_4$/EC-DEC, the impedance response of the $LiCoO_2$ cathode in the Nyquist plots has two semi-circles whose characteristic frequencies were observed at approximately 1 kHz and 1 Hz, and the impedance response of the graphite anode in the Nyquist plots has two semi-circles overlapping whose characteristic frequency was observed at approximately 1 kHz. As was the case with the 1 M $LiClO_4$/EC-DEC electrolyte, the charge transfer resistance of $LiCoO_2$ was approximately constant. The increase rate of the charge transfer resistance after 3, 6, and 24 hours are roughly calculated to be 1.2, 1.3, and 1.5, respectively. The increase rate of the charge transfer resistance of $LiCoO_2$ in the 1 M $LiClO_4$/EC-DEC electrolyte with H_2O was almost the same as that in the 1 M $LiClO_4$/EC-DEC electrolyte. The cobalt concentration in the 1 M $LiClO_4$/EC-DEC electrolyte with H_2O was nearly constant, as was the case with the 1 M $LiClO_4$/EC-DEC electrolyte, as shown in Fig. 4. Therefore, the result eliminates the suggestion that H_2O may affect the increase of the charge transfer resistance of $LiCoO_2$ and cobalt dissolution in the $LiClO_4$ electrolyte system. However, as is the case with the

electrolytes, the impedance of the graphite anode was unchanged at the frequency region in which the lithium migration in a SEI and the charge transfer occur.

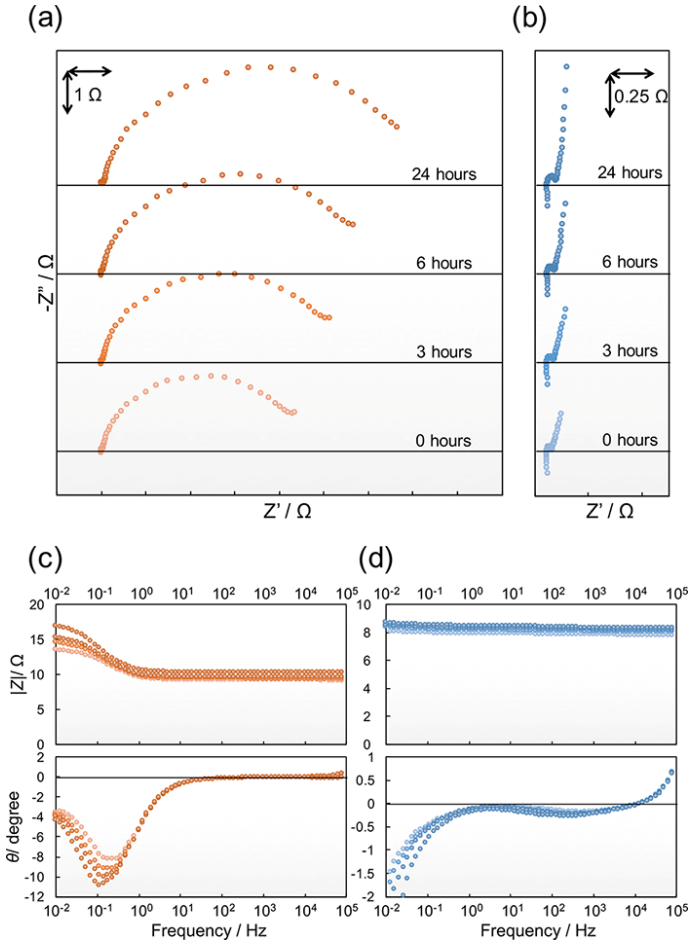

Figure 6. Nyquist and Bode plots of the impedances obtained in 1 M $LiClO_4$/EC-DEC with 50 ppm H_2O with elapsed time from the assembly of the (a) and (c) cathode symmetric cell, and (b) and (d) the anode symmetric cell.

The cobalt dissolution from the active material of $LiCoO_2$ was reported under storage at a high voltage [36]. However, even under storage at a lower voltage, approximately 3.7 V, the cobalt dissolution arising from HF attack of $LiCoO_2$ was observed, resulting in the increase of the charge transfer resistance of the $LiCoO_2$ cathode.

4. Conclusion

We consider the problem that the charge transfer resistance of $LiCoO_2$, with a potential of approximately 3.7 V, increased in the cathode symmetric cell, which we developed, with 1 M $LiPF_6$/EC-DEC electrolyte. The reason why the charge transfer resistance increased was investigated by EIS and ICP-MS analyses with various electrolyte solutions, which were 1 M $LiPF_6$/EC-DEC, 1 M $LiClO_4$/EC-DEC, 1 M $LiClO_4$/EC-DEC with 100 ppm of aqueous HF, and 1 M $LiClO_4$/EC-DEC with 50 ppm of H_2O. The increase of the charge transfer resistance of the $LiCoO_2$ cathode was

attributed to the cobalt dissolution from the active material of $LiCoO_2$. The cobalt dissolution from $LiCoO_2$ was revealed to occur even at low potentials in the presence of HF, which is generated from $LiPF_6$ and H_2O. The results indicate that avoidance of the HF generation is important for the analysis of LIB electrodes by using the separable cell. Therefore, the usability of the separable cell for the accurate analysis by means of EIS is enhanced.

Acknowledgments

This work was partly supported by the "Research & Development Initiative for Scientific Innovation of New Generation Batteries (RISING)" from the New Energy and Industrial Technology Development Organization (NEDO) of Japan.

Conflict of Interest

The authors declare no conflict of interest.

References

1. Nishi Y (2001) Lithium ion secondary batteries; past 10 years and the future. *J Power Sources* 100: 101–106.
2. Etacheri V, Marom R, Elazari R, et al. (2011) Challenges in the development of advanced Li-ion batteries: a review. *Energy Environ Sci* 4: 3243–3262.
3. Dunn B, Kamath H, Tarascon J-M (2011) Electrical energy storage for the grid: a battery of choices. *Science* 334: 928–935.
4. Yang Z, Zhang J, Kintner-Meyer MCW, et al. (2011) Electrochemical Energy Storage for Green Grid. *Chem Rev* 111: 3577–3613.
5. Broussely M, Biensan P, Bonhomme F, et al. (2005) Main aging mechanisms in Li ion batteries. *J Power Sources* 146: 90–96.
6. Vetter J, Novák P, Wagner MR, et al. (2005) Ageing mechanisms in lithium-ion batteries. *J Power Sources* 147: 269–281.
7. Smart MC, Ratnakumar BV (2011) Effects of Electrolyte Composition on Lithium Plating in Lithium-Ion Cells. *J Electrochem Soc* 158: A379–A389.
8. Aurbach D, Markovsky B, Salitra G, et al. (2007) Talyossef, M. Koltypin, et al., Review on electrode–electrolyte solution interactions, related to cathode materials for Li-ion batteries. *J Power Sources* 165: 491–499.
9. Aurbach D, Markovsky B, Rodkin A, et al. (2002) On the capacity fading of LiCoO2 intercalation electrodes. *Electrochimica Acta* 47: 4291–4306.
10. Takami N, Satoh A, Hara M, et al. (1995) Structural and Kinetic Characterization of Lithium Intercalation into Carbon Anodes for Secondary Lithium Batteries. *J Electrochem Soc* 142: 371–379.
11. Aurbach D, Levi MD, Levi E, et al. (1998) Common Electroanalytical Behavior of Li Intercalation Processes into Graphite and Transition Metal Oxides. *J Electrochem Soc* 145: 3024–3034.

12. Markovsky B, Levi MD, Aurbach D (1998) The basic electroanalytical behavior of practical graphite–lithium intercalation electrodes. *Electrochimica Acta* 43: 2287–2304.
13. Barsoukov E, Kim JH, Yoon CO, et al. (1999) Kinetics of lithium intercalation into carbon anodes: in situ impedance investigation of thickness and potential dependence. *Solid State Ionics*.
14. Zhang D, Haran BS, Durairajan A, et al. (2000) Studies on capacity fade of lithium-ion batteries. *J Power Sources* 91: 122–129.
15. Nagasubramanian G (2000) Two- and three-electrode impedance studies on 18650 Li-ion cells. *J Power Sources* 87: 226–229.
16. Li J, Murphy E, Winnick J, et al. (2001) Studies on the cycle life of commercial lithium ion batteries during rapid charge–discharge cycling. *J Power Sources* 102: 294–301.
17. Seki S, Kihira N, Mita Y, et al. (2011) AC Impedance Study of High-Power Lithium-Ion Secondary Batteries—Effect of Battery Size. *J Electrochem Soc* 158: A163–A166.
18. Mukoyama D, Momma T, Nara H, et al. (2012) Electrochemical Impedance Analysis on Degradation of Commercially Available Lithium Ion Battery during Charge–Discharge Cycling. *Chem Lett* 41: 444–446.
19. Osaka T, Momma T, Mukoyama D, et al. (2012) Proposal of novel equivalent circuit for electrochemical impedance analysis of commercially available lithium ion battery. *J Power Sources* 205: 483–486.
20. Hang T, Mukoyama D, Nara H, et al. (2013) Electrochemical impedance spectroscopy analysis for lithium-ion battery using Li4Ti5O12 anode. *J Power Sources* 222: 442–447.
21. Illig J, Ender M, Weber A, et al. (2015) Modeling graphite anodes with serial and transmission line models. *J Power Sources* 282: 335–347.
22. Hoshi Y, Narita Y, Honda K, et al. (2015) Optimization of reference electrode position in a three-electrode cell for impedance measurements in lithium-ion rechargeable battery by finite element method. *J Power Sources* 288: 168–175.
23. Osaka T, Mukoyama D, Nara H (2015) Review—Development of Diagnostic Process for Commercially Available Batteries, Especially Lithium Ion Battery, by Electrochemical Impedance Spectroscopy. *J Electrochem Soc* 162: A2529–A2537.
24. Osaka T, Nara H, Mukoyama D, et al. (2013) New Analysis of Electrochemical Impedance Spectroscopy for Lithium-ion Batteries. *J Electrochem Sci Tech* 4: 157–162.
25. Mendoza-Hernandez OS, Ishikawa H, Nishikawa Y, et al. (2014) State of Charge Dependency of Graphitized-Carbon-Based Reactions in a Lithium-ion Secondary Cell Studied by Electrochemical Impedance Spectroscopy. *Electrochimica Acta* 131: 168–173.
26. Bünzli C, Kaiser H, Novák P (2015) Important Aspects for Reliable Electrochemical Impedance Spectroscopy Measurements of Li-Ion Battery Electrodes. *J Electrochem Soc* 162: A218–A222.
27. Yokoshima T, Nara H, Mukoyama D, et al. (2011) Performance of Fine Reference Electrode in Thin Laminated Li-Ion Cell, in: Meet. Abstr, The Electrochemical Society, pp. 1451–1451.
28. Jansen AN, Dees DW, Abraham DP, et al. ((2007)) Low-temperature study of lithium-ion cells using a LiySn micro-reference electrode. *J Power Sources* 174: 373–379.
29. La Mantia F, Wessells CD, Deshazer HD, et al. (2013) Reliable reference electrodes for lithium-ion batteries. *Electrochem Commun* 31: 141–144.
30. Gómez-Cámer JL, Novák P (2013) Electrochemical impedance spectroscopy: Understanding the role of the reference electrode. *Electrochem Commun* 34: 208–210.

31. Adler SB (2002) Reference Electrode Placement in Thin Solid Electrolytes. *J Electrochem Soc* 149: E166–E172.
32. Klink S, Höche D, La Mantia F, et al. (2013) FEM modelling of a coaxial three-electrode test cell for electrochemical impedance spectroscopy in lithium ion batteries. *J Power Sources* 240: 273–280.
33. Momma T, Yokoshima T, Nara H, et al. (2014) Distinction of impedance responses of Li-ion batteries for individual electrodes using symmetric cells. *Electrochimica Acta* 131: 195–201.
34. Chen CH, Liu J, Amine K (2001) Symmetric cell approach and impedance spectroscopy of high power lithium-ion batteries. *J Power Sources* 96: 321–328.
35. Levi MD, Dargel V, Shilina Y, et al. (2014) Impedance Spectra of Energy-Storage Electrodes Obtained with Commercial Three-Electrode Cells: Some Sources of Measurement Artefacts. *Electrochimica Acta* 149: 126–135.
36. Amatucci G (1996) Cobalt dissolution in LiCoO2-based non-aqueous rechargeable batteries. *Solid State Ionics* 83: 167–173.
37. Levi MD, Salitra G, Markovsky B, et al. (1999) Solid-State Electrochemical Kinetics of Li-Ion Intercalation into Li1 − x CoO2: Simultaneous Application of Electroanalytical Techniques SSCV, PITT, and EIS. *J Electrochem Soc* 146: 1279–1289.
38. Momma T, Matsunaga M, Mukoyama D, et al. (2012) Ac impedance analysis of lithium ion battery under temperature control. *J Power Sources* 216: 304–307.
39. Nara H, Mukoyama D, Yokoshima T, et al. (2016) Impedance Analysis with Transmission Line Model for Reaction Distribution in a Pouch Type Lithium-Ion Battery by Using Micro Reference Electrode. *J Electrochem Soc* 163: A434–A441.

AIMS Press